

## **STABILIZATION OF ROAD SUBGRADE UTILIZING LADLE REFINED FURNACE SLAG**

**Rohit Saha<sup>1</sup>, Md Tausifur Rahman Mollik<sup>2</sup> and Mohammed Russedul Islam<sup>\*3</sup>**

<sup>1</sup> Graduate Student, Military Institute of Science and Technology, Bangladesh, e-mail: [rohitsahamist@gmail.com](mailto:rohitsahamist@gmail.com)

<sup>2</sup> Undergraduate Student, Military Institute of Science and Technology, Bangladesh, e-mail: [zisan.mollik2001@gmail.com](mailto:zisan.mollik2001@gmail.com)

<sup>3</sup> Associate Professor, Military Institute of Science and Technology, Bangladesh, e-mail: [russed@ce.mist.ac.bd](mailto:russed@ce.mist.ac.bd)

**\*Corresponding Author**

### **ABSTRACT**

Soil stabilization is essential for improving the stability and strength of weak subgrade soils. This study investigates the potential of utilizing Ladle refined furnace (LRF) slag, a steel manufacturing by-product, as a promising stabilizer for strengthening subgrade soil. A series of laboratory experiments were conducted to determine Atterberg limits, free swell index, and unconfined compressive strength. The untreated soil, classified as Clay of High Plasticity (CH), observed a liquid limit (LL) of 54% and a plasticity index (PI) of 33% and is classified as moderately expansive soil according to the Austroads Guide to Pavement Technology. After stabilization with LRF slag, the LL decreased from 54% to 40%, and the PI reduced from 33% to 16%. Moreover, the soil turned from CH to ML (Silt of Low Plasticity), indicating a substantial improvement in workability. The incorporation of 15% LRF slag resulted in a 73% and 82% reduction in the free swelling index after 1 day and 7 days of aging, respectively. Unconfined compressive strength improved by 335% from 0.17 MPa to 0.74 MPa at an optimum LRF slag content of 15%. Additionally, stress-strain behavior showed a transition from ductile to brittle behavior with the addition of LRF slag. These findings confirm that LRF slag, an industrial by-product, can serve as an effective stabilizer for expansive soils, significantly improving strength and reducing plasticity and swelling potential.

**Keywords:** *Subgrade Stabilization, industrial waste, consistency, strength, free swelling index.*

## **1. INTRODUCTION**

The construction of durable and sustainable road infrastructure is a vital aspect of civil engineering practice. In the context of Bangladesh, where rapid urbanization and infrastructure development are generating increasing amounts of industrial waste, the reuse of such by-products in civil engineering applications presents a practical and sustainable solution. The country faces significant challenges in managing industrial by-products, with steel production contributing to the accumulation of slag. Ladle Refined Furnace (LRF) slag is a secondary by-product generated during the production of steel (Islam et al., 2024). Another study (Maghool et al., 2017; Skaf et al., 2016) demonstrated that producing one ton of steel yields roughly 30–80 kg of LRF slag, while (Mahoutian & Shao, 2016) estimated the annual global generation at approximately 30 million tons. In Bangladesh, the annual steel consumption is around four million tonnes, produced by approximately 400 steel mills (Ahmad & Rahman, 2018). Generally, this slag is disposed in landfills (Borges Marinho et al., 2017; Rodriguez et al., 2009), which creates environmental and land depletion challenges.

To address these issues and promote sustainability, researchers have explored various alternative applications for LRF slag by taking advantage of its favorable physicochemical characteristics. As a result, LRF slags have been investigated for many civil engineering and industrial uses, such as inclusion in construction mortar mixes (Herrero et al., 2016; Rodriguez et al., 2009; Santamaría-Vicario et al., 2015), as fast-hardening binders including cement and concrete materials (Adesanya et al., 2017; Kim et al., 2016; Najm et al., 2021), and as mineral aggregates in plaster production (Rodríguez et al., 2013). It has also been applied in soil-cement mixtures for road pavements (Manso et al., 2005) and in embankment construction (Montenegro et al., 2013).

Overall, these findings highlight that LRF slag is not simply an industrial waste but a valuable secondary resource with diverse civil and environmental engineering applications, contributing to circular economy and sustainability goals. In addition, the previous studies found that the mineral composition of LRF slag is mainly composed of C3S, C2S, C2F, and f-CaO (Yang et al., 2025). It can be seen that the composition of LRF slag is similar to that of Portland cement clinker, and it is a cementitious material with potential gel characteristics (Rui et al., 2022). Another study (Islam et al., 2024) showed that the unconfined compressive strength of clayey soil increased by 219% upon the inclusion of LRF slag and improved California Bearing Ratio (CBR) values significantly, indicating its effectiveness in improving load-bearing capacity. Laboratory studies demonstrate that adding 5–20% steel slag to expansive clays significantly reduces liquid limit and swelling pressure while increasing dry density, Unconfined Compressive Strength (UCS), and soaked CBR values (Abdalqadir et al., 2020; Zumrawi & Babikir, 2017).

Insufficient research exists on the swelling behavior of expansive soil treated with LRF slag. In particular, the impact of cured and uncured conditions on swelling behavior remains unexplored. This study aims to fill that existing gap in literature by evaluating the free swelling index. After a curing period of 1 and 7 days, respectively. Moreover, changes in Atterberg limits indicate that the transition in the consistency and plasticity characteristics of expansive soil after stabilization with LRF slag has not yet been thoroughly explored. Additionally, this study investigates the shift in soil unconfined compressive strength after stabilization with LRF slag.

## **2. METHODOLOGY**

Representative soil samples were collected from a problematic subgrade site and tested for grain size distribution, specific gravity, and Atterberg limit to determine their basic geotechnical properties. The soil was then mixed with LRF slag in the proportions of 5%, 10%, 15%, and 20% according to dry weight. Standard Proctor tests were conducted to determine optimum moisture content (OMC) and maximum dry density (MDD).

To evaluate the improvement in strength, unconfined compressive strength (UCS) tests were conducted on specimens cured for seven days. Each specimen was subjected to static compression in three uniform layers within a cylindrical mold. After the compaction, the compacted sample was promptly sealed in plastic wrap and thereafter placed in a standard chamber for curing. Following a curing period of 7 days at a relative humidity of 95% and a temperature of  $23\pm 2^{\circ}\text{C}$ , the samples underwent unconfined

compression testing in accordance with ASTM D2166. The Atterberg limits (liquid limit, plastic limit, and plasticity index) were determined in accordance with ASTM D4318. The liquid limit (LL) was determined using the Casagrande apparatus, the plastic limit (PL) was acquired by rolling soil threads to a diameter of 3 mm, and the plasticity index (PI) was computed as the difference between LL and PL. The Atterberg limit test was conducted to assess the change in plasticity of the soil due to slag addition. Furthermore, the Free Swell Index (FSI) test was conducted on both untreated and stabilized soils mixed with 5%, 10%, 15%, and 20% LRF slag to investigate the decrease in swelling potential with increasing slag content. The Free Swell Index (FSI) procedure was performed as per (IS 2720-40) to ensure accuracy and consistency. However, 10 g of oven-dried sample passing through a 425- $\mu$ m sieve was immersed in both water and kerosene, and the volumetric increase in water was recorded to evaluate the soil's swelling potential. All the laboratory tests were performed according to respective ASTM codes, including particle size analysis (ASTM D6913), hydrometer analysis (ASTM D7928), specific gravity test (ASTM D854), Standard Proctor compaction (ASTM D698). Figure 1 represents the flowchart of the study.

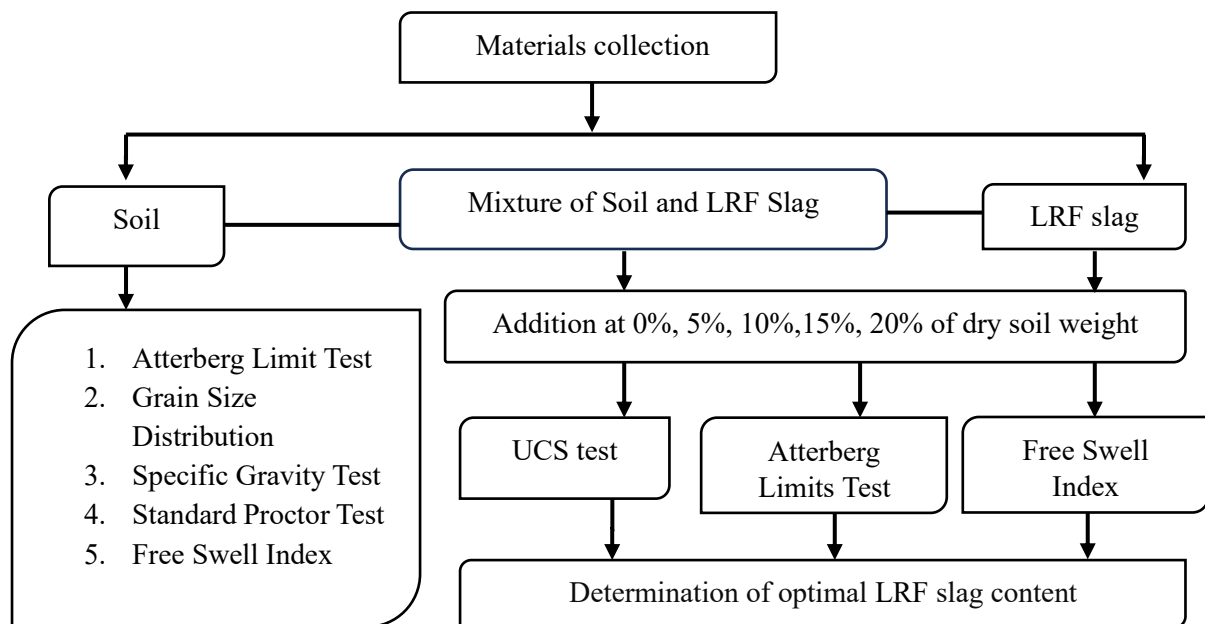


Figure 1: Flowchart of the study

### 3. RESULTS AND DISCUSSION

#### 3.1 Soil Characteristics

According to the Unified Soil Classification System, the soil contains approximately 91% silt and clay particles, as shown in Figure 2 (ASTM D2487–11), and classified as inorganic clays of high plasticity (CH).

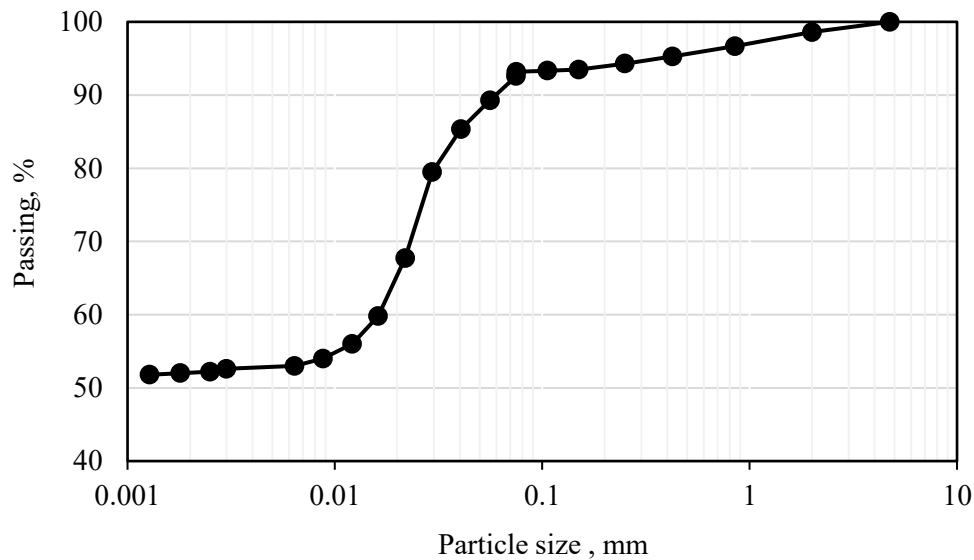


Figure 2: Particle size distribution curve of soil

Table 1 presents the geotechnical properties for the soil sample. The soil exhibits a liquid limit of 54% and a plasticity index of 33%, which shows medium plasticity.

Table 1: Engineering properties of the soil

Property		Value
Specific gravity		2.68
Atterberg limits	Liquid limit, %	54
	Plastic limit, %	21
	Plasticity index, %	33
Compaction parameters	Max dry density, gm/cm <sup>3</sup>	1.70
	Optimum moisture content, %	18.1

### 3.2 Effect of LRF Slag on Atterberg limits

The LL, PL, and PI of untreated soil are 53.6%, 21.1%, and 32.5%, respectively. Incorporating 0% to 20% LRF into the expansive soil resulted in a 28.1% reduction in liquid limit and increased the PL by 21.6%, as shown in figure 3. This change is attributed to the compression of the double diffusion layer caused by the exchange of monovalent ions with divalent calcium ions ( $Ca^{2+}$ ) from LRF (Han et al., 2021). This process reduces repulsive forces between clay particles, lowers water retention (lower LL), and increases plastic limit. This mechanism aligns with the findings of (Espinosa et al., 2023), who observed similar changes in clayey soils stabilized with ladle furnace slag, attributing the behavior to diffuse double layer compression and enhanced interparticle bonding.

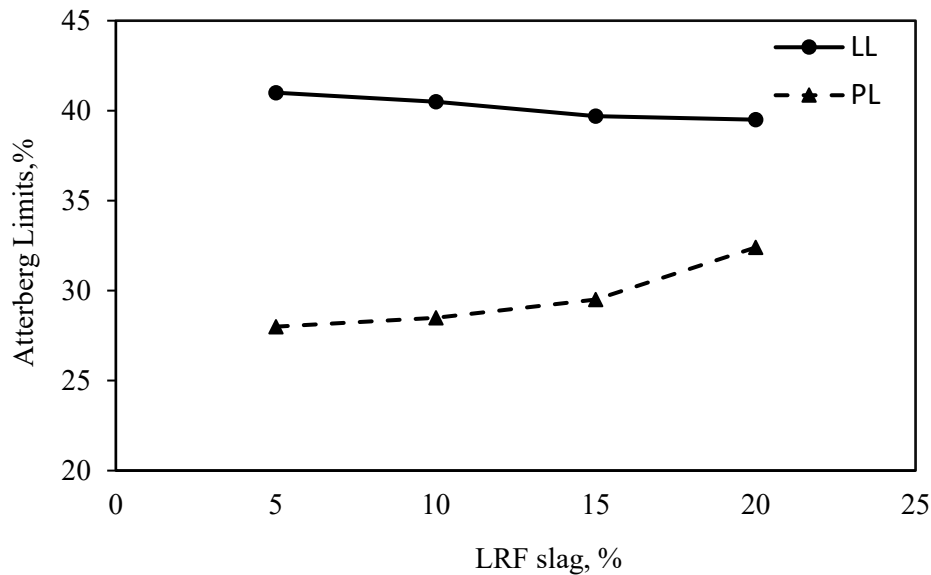


Figure 3: Variation of Atterberg limits with different LRF contents

### 3.3 Effect of LRF Slag in Soil Behavior

Figure 4 is a plasticity chart (Casagrande chart) that illustrates the relationship between the Liquid Limit (LL) on the horizontal axis and the Plasticity Index (PI) on the vertical axis. It uses Atterberg limits to identify the soil types. The liquid limit (LL) of clay soil is 54%, which falls within the range of 50%–70%, and the plasticity index (PI) is 33%, which falls within the range of 25%–45%. These values correspond to the Austroad classification (Austroads, 2017) for moderately expansive soils. The green square shows the untreated soil, which is in the CH or MH zone, as shown in Figure 4, indicating high plasticity clay or silt. When mixed with different percentages of LRF slag, the soil samples move to the left and downward. The liquid limit decreases to 38%, and the plasticity index decreases to 6%. According to criteria of Austroad (Moffatt, 2017), soils with  $LL < 50\%$  and  $PI < 25\%$  are considered to have low expansion. These treated soil samples fall in the ML zone, showing a transition to a low-plasticity silt soil type.

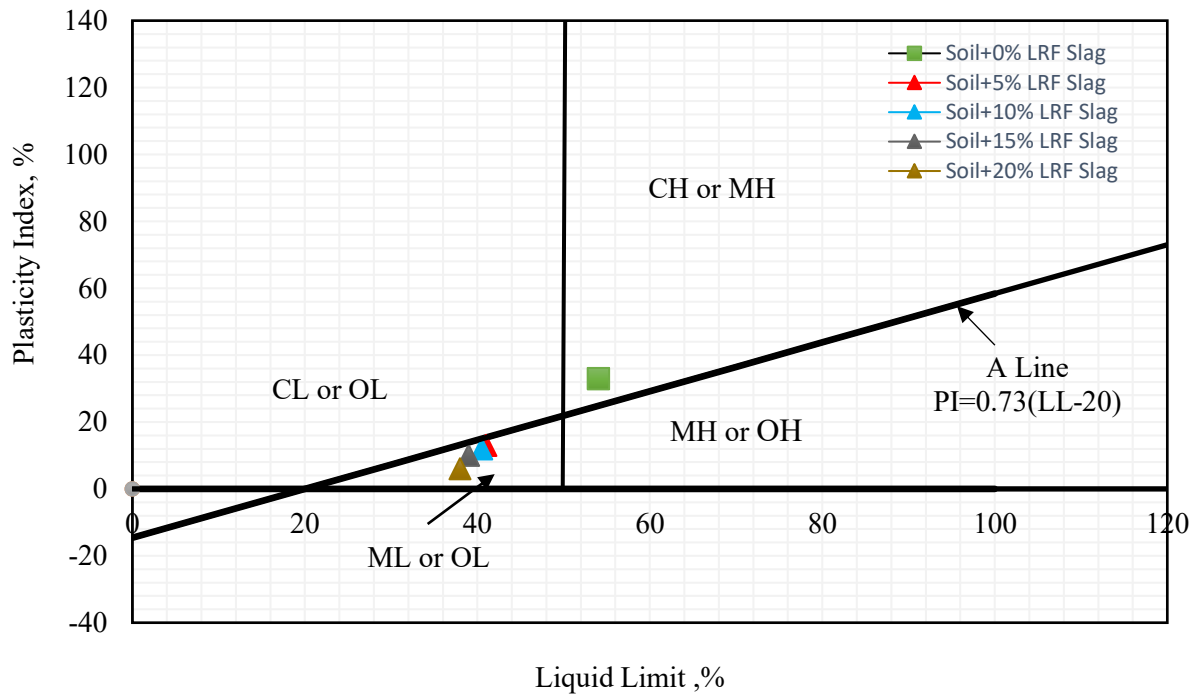


Figure 4: variation of USCS soil classification with different LRF contents

### 3.4 Effect of LRF Slag on Strength

The unconfined compressive strength (UCS) of soil samples stabilized with different proportions of LRF slag (0%, 5%, 10%, 15%, and 20%) was determined. Soil-LRF slag mixtures were prepared following the standard Proctor compaction procedure at optimum moisture content (OMC) of 18.1%. As shown in Figure 5, the addition of LRF slag increased the UCS values up to 15%, after which a decline was observed. The UCS of the soil increased from 0.17 MPa for the untreated sample to 0.74 MPa for the sample containing 15% LRF slag after 7 days of curing. The increase in strength of LRF slag by 15% is due to pozzolanic reactions between calcium oxide (CaO) present in the slag and reactive silica in the clay soil, leading to the formation of cementitious compounds (Kang et al., 2024). These compounds enhance interparticle bonding and significantly improve the UCS of stabilized soils. At 20% LRF content, the unconfined compressive strength decreases due to insufficient reactive silica in the soil to interact with the additional calcium oxide from the 20% LRF slag. As a result, unreacted slag particles remained in the clay matrix and decreased interparticle bonding, leading to reduced strength.

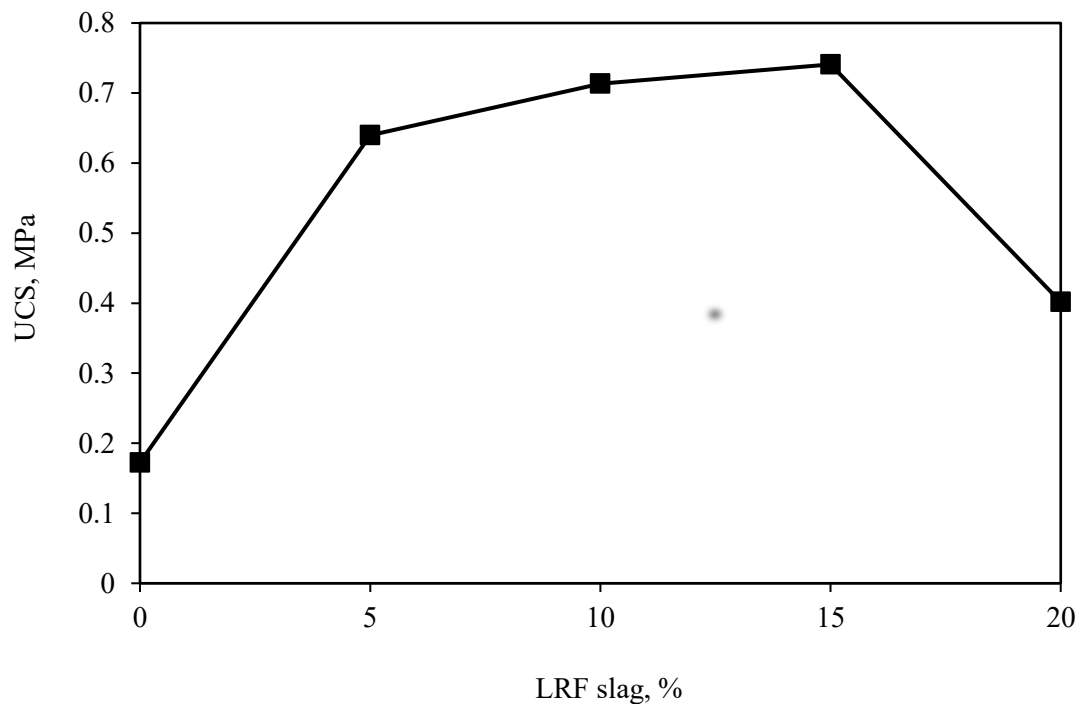


Figure 5: Variation of UCS with different LRF contents

### 3.5 Effect of LRF Slag on Stress- Strain Behavior

Figure 6 illustrates the transition from ductile to brittle behavior with varying proportions of LRF slag in soil. Untreated soil shows minimal stress capacity (0.17 MPa), while additions of LRF slag (5%, 10%, 15%, and 20%) gradually increase strength. The best performance is observed for 15% LRF slag combined with soil, which reaches the highest peak stress of 0.74 MPa at around 6.42% strain, demonstrating the optimal mix for strength. At 20% LRF slag content, ductility increases because the slag exceeds the optimum level for effective pozzolanic reactions. When excess slag is present, a significant portion remains unreacted due to insufficient available reactive silica from the soil. Instead of forming cementitious phases, this excess amount of slag remains unreacted, reducing the stiffness of the soil matrix. Because of this, the mixture has a lower peak strength but a higher strain capacity, which makes it more ductile. Thus, the graph reveals a critical point where the mixture shifts from ductile to brittle behavior depending on LRF slag content.

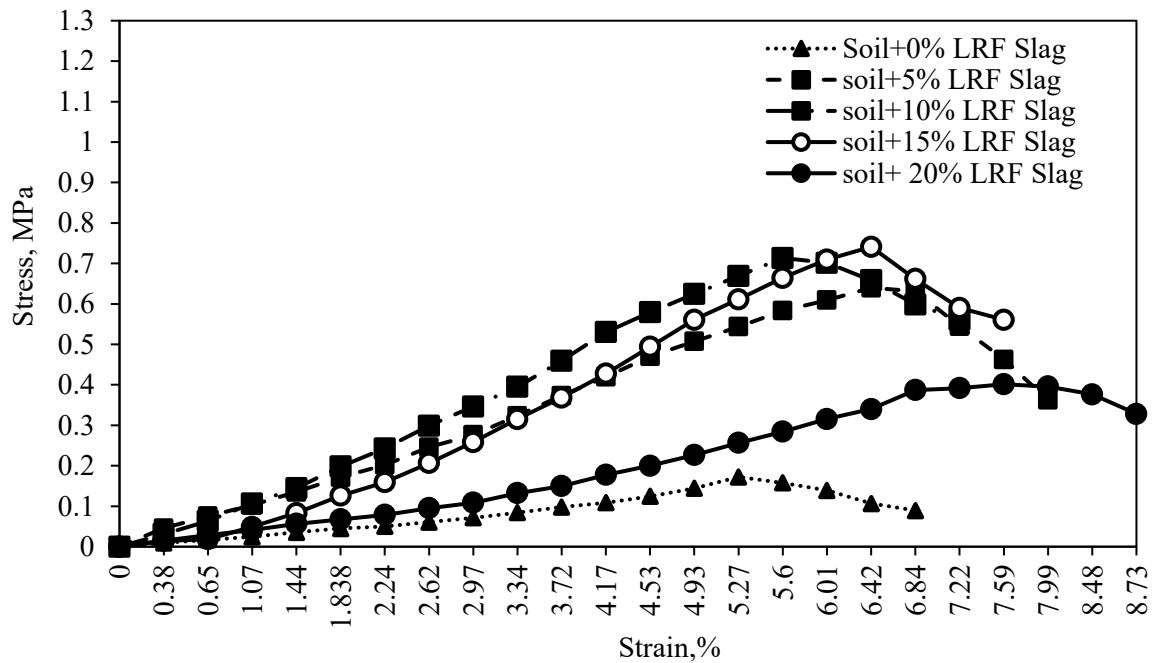


Figure 6: Variation of stress-strain curves of samples with different LRF contents

### 3.6 Effect of LRF Slag on Free Swell Index

The FSI of the untreated soil sample was found to be 35%, as shown in Figure 7. A report demonstrated that the FSI ranges from 20 to 35 and can be classified the degree of expansiveness as medium (Singh Randhawa et al., 2022). A slight decrease in FSI was observed with increase in LRF slag content after 1 day of curing. This initial reduction is likely due to the initial cation exchange reactions between the calcium oxide (CaO) present in the LRF slag and silica present in the clay minerals, which initiate pozzolanic activity. A more pronounced decrease in FSI was observed after curing for 7 days due to the progressive generation of cementitious phases, which bind clay particles together and suppress the expansive behavior of clay minerals. The reduction in swelling capacity can also be explained by diffuse double layer compression through cation exchange as well as increased particle bonding as a result of the generation of cementitious compounds that strengthen and stabilize the clay matrix (Han et al., 2021). Similar observations were reported by a study (Inas et al., 2021), where adding 8% paper ash to clay soil reduced FSI from 60% to 11%.

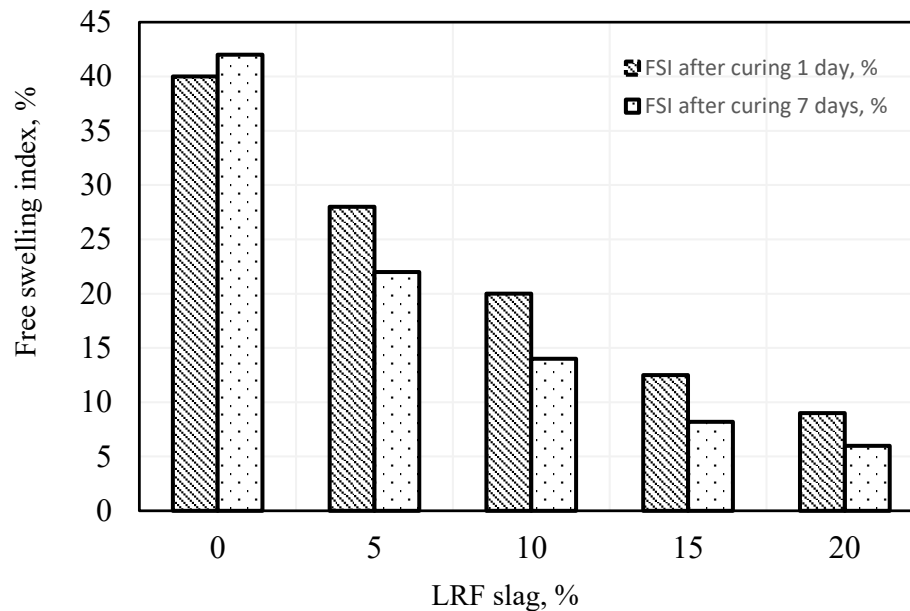


Figure 7: Variation of free swelling index of samples with different LRF contents

#### 4. CONCLUSIONS

This study explores the effectiveness of ladle refining furnace (LRF) slag as a sustainable stabilizing material for clay soil. A systematic experimental program was conducted to assess the effect of LRF slag on the soil characteristics, including unconfined compressive strength (UCS), free swell index (FSI), and Atterberg limits. The main findings of the study are summarized as follows:

- i. After stabilization with LRF slag, the liquid limit decreased from 54% to 40%, while the plasticity index decreased from 33% to 16%. This significant reduction in plasticity parameters changed the classification of the soil from CH (high plasticity clay) to ML (low plasticity silt), demonstrating a substantial increase in its workability and suitability of the soil for road subgrade applications.
- ii. The unconfined compressive strength (UCS) of the untreated soil was found to be 0.172 MPa, which increased more than four times to 0.741 MPa with 15% LRF. The 15% LRF slag refers to the most substantial improvement in soil strength among various LRF contents. With 20% LRF slag constitution, the UCS was found to drop to 0.4018 MPa, indicating a reduction in strength.
- iii. From the stress-strain graph it is observed that as the percentage of LRF slag content increases up to 15%, the clay moves from ductile to brittle behavior. However, at 20% LRF slag content, the ductility increases again, showing an opposite trend.
- iv. Incorporation of 15% LRF slag reduced the free swell index (FSI) by approximately 74% and 83% after curing for 1 and 7 days, respectively. This substantial reduction reflects the high efficiency of the LRF slag in reducing clay expansion, which is attributed to the progressive pozzolanic interactions that develop with extended curing time.

In summary, the findings of this study demonstrate that LRF slag can be effectively used to stabilize expansive soils, promoting sustainable waste management practices. However, the present study did not consider any field application of the proposed stabilization technique, and will be extended in future research. Additionally, the mechanisms contributing to strength development require further detailed investigation.

## **ACKNOWLEDGMENTS**

The authors sincerely acknowledge the Department of Civil Engineering, Military Institute of Science and Technology, Dhaka, for their invaluable support in providing the laboratory facilities required for this study and the technical support needed to conduct it. The authors sincerely acknowledge Bangladesh Steel Re-Rolling Mills (BSRM) for their kind cooperation in supplying the Ladle Refining Furnace (LRF) slag utilized in this study.

## **Declaration of Use of AI:**

The authors declare that this manuscript was prepared entirely by the authors without the use of artificial intelligence (AI) tools in the writing, editing, analysis, or preparation of this manuscript.

## **REFERENCES**

- Abdalqadir, Z. K., Salih, N. B., & Salih, S. J. H. (2020). Using Steel Slag for Stabilizing Clayey Soil in Sulaimani City-Iraq. *Journal of Engineering*, 26(7), 145–157. <https://doi.org/10.31026/j.eng.2020.07.10>
- Adesanya, E., Ohenoja, K., Kinnunen, P., & Illikainen, M. (2017). Alkali Activation of Ladle Slag from Steel-Making Process. *Journal of Sustainable Metallurgy*, 3(2), 300–310. <https://doi.org/10.1007/s40831-016-0089-x>
- Ahmad, S. I., & Rahman, Md. S. (2018). Mechanical and Durability Properties of Induction-Furnace-Slag-Incorporated Recycled Aggregate Concrete. *Advances in Civil Engineering*, 2018(1). <https://doi.org/10.1155/2018/3297342>
- Borges Marinho, A. L., Mol Santos, C. M., Carvalho, J. M. F. de, Mendes, J. C., Brigolini, G. J., & André Fiorotti Peixoto, R. (2017). Ladle Furnace Slag as Binder for Cement-Based Composites. *Journal of Materials in Civil Engineering*, 29(11). [https://doi.org/10.1061/\(ASCE\)MT.1943-5533.0002061](https://doi.org/10.1061/(ASCE)MT.1943-5533.0002061)
- Designation: D 698-07 Standard Test Methods for Laboratory Compaction Characteristics of Soil Using Standard Effort (12 400 ft-lbf/ft<sup>3</sup> (600 kN-m/m<sup>3</sup>)) 1. (n.d.). <https://store.astm.org/d0698-12r21.html>
- Espinosa, A. B., Revilla-Cuesta, V., Skaf, M., Serrano-López, R., & Ortega-López, V. (2023). Strength performance of low-bearing-capacity clayey soils stabilized with ladle furnace slag. *Environmental Science and Pollution Research*, 30(45), 101317–101342. <https://doi.org/10.1007/s11356-023-29375-y>
- Han, S., Wang, B., Gutierrez, M., Shan, Y., & Zhang, Y. (2021). Laboratory Study on Improvement of Expansive Soil by Chemically Induced Calcium Carbonate Precipitation. *Materials*, 14(12), 3372. <https://doi.org/10.3390/ma14123372>
- Herrero, T., Vegas, I. J., Santamaría, A., San-José, J. T., & Skaf, M. (2016). Effect of high-alumina ladle furnace slag as cement substitution in masonry mortars. *Construction and Building Materials*, 123, 404–413. <https://doi.org/10.1016/j.conbuildmat.2016.07.014>
- Inas, B., Salah, M., Riad, B., & Imane, I. (2021). Treatment of clay soil with paper ash. *Selected Scientific Papers - Journal of Civil Engineering*, 16(2), 163–174. <https://doi.org/10.2478/sspjce-2021-0024>
- Indian Standards, B. (n.d.). IS 2720-40 (1977): Methods of test for soils, Part 40: Determination of free swell index of soils.

- International, A., & indexed by mero, files. (n.d.-a). *Specific Gravity of Soil Solids by Water Pycnometer I*.
- International, A., & indexed by mero, files. (n.d.-b). *Standard Test Method for Unconfined Compressive Strength of Cohesive Soil I*.
- Islam, S., Ara, S., & Islam, J. (2024). An experimental investigation on utilization of ladle refined furnace (LRF) slag in stabilizing clayey soil. *Heliyon*, 10(4), e26004. <https://doi.org/10.1016/j.heliyon.2024.e26004>
- Kang, X., Li, C., Zhang, M., Yu, X., & Chen, Y. (2024). Mechanical Properties and Stabilization Mechanism of Steel Slag-Rice Husk Ash Solidified High Plasticity Clay. *Geotechnical Testing Journal*, 47(1). <https://doi.org/10.1520/GTJ20220294>
- Kim, J.-M., Choi, S.-M., & Han, D. (2016). Improving the mechanical properties of rapid air cooled ladle furnace slag powder by gypsum. *Construction and Building Materials*, 127, 93–101. <https://doi.org/10.1016/j.conbuildmat.2016.09.102>
- Maghool, F., Arulrajah, A., Horpibulsuk, S., & Du, Y.-J. (2017). Laboratory Evaluation of Ladle Furnace Slag in Unbound Pavement-Base/Subbase Applications. *Journal of Materials in Civil Engineering*, 29(2). [https://doi.org/10.1061/\(ASCE\)MT.1943-5533.0001724](https://doi.org/10.1061/(ASCE)MT.1943-5533.0001724)
- Mahoutian, M., & Shao, Y. (2016). Low temperature synthesis of cement from ladle slag and fly ash. *Journal of Sustainable Cement-Based Materials*, 5(4), 247–258. <https://doi.org/10.1080/21650373.2015.1047913>
- Manso, J. M., Losañez, M., Polanco, J. A., & Gonzalez, J. J. (2005). Ladle Furnace Slag in Construction. *Journal of Materials in Civil Engineering*, 17(5), 513–518. [https://doi.org/10.1061/\(ASCE\)0899-1561\(2005\)17:5\(513\)](https://doi.org/10.1061/(ASCE)0899-1561(2005)17:5(513))
- Moffatt, Michael. (2017). *Guide to pavement technology part 2 : pavement structural design Michael Moffatt*. Austroads LTD.
- Montenegro, J. M., Celemín-Matachana, M., Cañizal, J., & Setién, J. (2013). Ladle Furnace Slag in the Construction of Embankments: Expansive Behavior. *Journal of Materials in Civil Engineering*, 25(8), 972–979. [https://doi.org/10.1061/\(ASCE\)MT.1943-5533.0000642](https://doi.org/10.1061/(ASCE)MT.1943-5533.0000642)
- Najm, O., El-Hassan, H., & El-Dieb, A. (2021). Ladle slag characteristics and use in mortar and concrete: A comprehensive review. *Journal of Cleaner Production*, 288, 125584. <https://doi.org/10.1016/j.jclepro.2020.125584>
- Practice for Classification of Soils for Engineering Purposes (Unified Soil Classification System). (2017). ASTM International. <https://doi.org/10.1520/D2487-17>
- Rodríguez, A., Gutiérrez-González, S., Horgnies, M., & Calderón, V. (2013). Design and properties of plaster mortars manufactured with ladle furnace slag. *Materials & Design (1980-2015)*, 52, 987–994. <https://doi.org/10.1016/j.matdes.2013.06.041>
- Rodriguez, Á., Manso, J. M., Aragón, Á., & Gonzalez, J. J. (2009). Strength and workability of masonry mortars manufactured with ladle furnace slag. *Resources, Conservation and Recycling*, 53(11), 645–651. <https://doi.org/10.1016/j.resconrec.2009.04.015>
- Rui, Y., Qian, C., Zhang, X., & Ma, Z. (2022). Different carbon treatments for steel slag powder and their subsequent effects on properties of cement-based materials. *Journal of Cleaner Production*, 362, 132407. <https://doi.org/10.1016/j.jclepro.2022.132407>
- Santamaría-Vicario, I., Rodríguez, A., Gutiérrez-González, S., & Calderón, V. (2015). Design of masonry mortars fabricated concurrently with different steel slag aggregates. *Construction and Building Materials*, 95, 197–206. <https://doi.org/10.1016/j.conbuildmat.2015.07.164>
- Singh Randhawa, K., Chauhan, R., & Kumar, R. (2022). An investigation on the effect of lime addition on UCS of Indian black cotton soil. *Materials Today: Proceedings*, 50, 797–803. <https://doi.org/10.1016/j.matpr.2021.05.586>
- Skaf, M., Ortega-López, V., Fuente-Alonso, J. A., Santamaría, A., & Manso, J. M. (2016). Ladle furnace slag in asphalt mixes. *Construction and Building Materials*, 122, 488–495. <https://doi.org/10.1016/j.conbuildmat.2016.06.085>

- Standard Test Methods for Particle-Size Distribution (Gradation) of Soils Using Sieve Analysis 1. (n.d.). <https://doi.org/10.1520/D6913-17>
- Test Method for Particle-Size Distribution (Gradation) of Fine-Grained Soils Using the Sedimentation (Hydrometer) Analysis. (2017). ASTM International. <https://doi.org/10.1520/D7928-17>
- Test Methods for Liquid Limit, Plastic Limit, and Plasticity Index of Soils. (2017). ASTM International. <https://doi.org/10.1520/D4318-17E01>
- Yang, M., Yan, Z., & Li, Z. (2025). Revealing the tricalcium silicate formation behaviors in modified EAF slag at high temperatures for the production of electric recycled cement. *Cement and Concrete Research*, 189, 107756. <https://doi.org/10.1016/j.cemconres.2024.107756>
- Zumrawi, M. M. E., & Babikir, A. A.-A. A. (2017). Laboratory Study of Steel Slag Used in Stabilizing Expansive Soil. *Asian Engineering Review*, 4(1), 1–6. <https://doi.org/10.20448/journal.508.2017.41.1.6>